Available online at www.sciencedirect.com

ScienceDirect

Geochimica et Cosmochimica Acta 217 (2017) 349–364

Geochimica et Cosmochimica Acta

www.elsevier.com/locate/gca

Olivinites in the angrite D'Orbigny: Vestiges of pristine reducing conditions during angrite formation

M.E. Varela [a,*], S.-L. Hwang [b], P. Shen [c], H.-T. Chu [d], T.-F. Yui [e], Y. Iizuka [e], F. Brandstätter [f], Y.A. Abdu [g]

[a] *Instituto de Ciencias Astronómicas de la Tierra y del Espacio (ICATE), Avenida España 1512 sur, J5402DSP San Juan, Argentina*
[b] *Department of Materials Science and Engineering, National Dong Hwa University, Hualien, Taiwan, ROC*
[c] *Department of Materials and Optoelectronic Science, National Sun Yat-sen University, Kaohsiung, Taiwan, ROC*
[d] *Central Geological Survey, PO Box 968, Taipei, Taiwan, ROC*
[e] *Institute of Earth Sciences, Academia Sinica, Taipei, Taiwan, ROC*
[f] *Mineralogisch-Petrographische Abteilung, Naturhistorisches Museum, Burgring 7, 1010 Wien, Austria*
[g] *Department of Applied Physics and Astronomy, University of Sharjah, P.O. Box 27272, Sharjah, United Arab Emirates*

Received 4 September 2016; accepted in revised form 12 August 2017; available online 20 August 2017

Abstract

Olivinites, together with olivine megacrysts, are the most magnesian phases found in angrites. Their chemical composition (mg# 90) is out of equilibrium with the groundmass and far away from that of possible precipitates from angrite parent melts. Therefore olivinites, as well as olivine megacrysts, were considered as xenoliths and xenocrysts. We report here a detailed study of five olivinites from the angrite D'Orbigny. Our results indicate that D'Orbigny experienced metasomatic alteration processes, which led to enrichments in FeO and MnO (relative to the original composition), changing the initial Mg-rich composition of the olivines to the one seen now. As this process took place in equilibrium with a chondritic reservoir (e.g., Fe/Mn ratios spreading around primitive values), the primitive (Mg-rich) olivine chemical composition was changed towards a more fayalitic one while preserving a chondritic signature. This chondritic signature was preserved in the Fe/Mn ratio of the olivinites, olivine megacrysts, augite grains in olivinites and groundmass olivine of D'Orbigny. Therefore the fayalite content of about 35 mol.% that characterizes the groundmass olivine of this rock – as well as other angrites-does not correspond to its original composition but may be the result of a late metasomatic process that affected these rocks. If so, olivinites and Mg-rich olivines might not be compositionally exotic phases but are an early constituent phase that retained the pristine more reducing conditions that have been preserved in some angrites, where they form either a small part of the rock (e.g., Asuka 881371 and D'Orbigny) or the majority of it (NWA 8535).

Keywords: Angrites; Olivinites; D'Orbigny

1. INTRODUCTION

Angrites are a small group of achondrite meteorites as old as the solar system; as indicated by their Pb-Pb ages (e.g., LEW Cliff 86010: 4558.55 ± 0.15 Ma and D'Orbigny: 4563.36 ± 0.34 Ma) (Amelin, 2008; Brennecka et al., 2010). They are the most alkali-depleted rocks in the Solar System (e.g., Warren and Kallemeyn, 1995; Warren et al., 1995), with little evidence for shock and impact brecciation. Although angrites are widely believed to be igneous rocks of basaltic composition originating from a differentiated planetesimal (e.g., Treiman, 1989; Mittlefehldt and

* Corresponding author.
E-mail address: eugeniavarela@conicet.gov.ar (M.E. Varela).

http://dx.doi.org/10.1016/j.gca.2017.08.027
0016-7037/

Lindstrom, 1990; Longhi, 1999; Mittlefehldt et al., 2002), the source of angritic liquids remains unknown. In the case of D'Orbigny, Kurat et al. (2004) and Varela et al. (2003 and 2005), suggested that the genesis of this particular rock appears to be more akin to that of chondritic constituents like CAIs than to that of planetary differentiated rocks. Therefore, the genesis of these rocks is controversial and no consensus has yet been reached.

Based on ^{26}Al energy considerations Schiller et al. (2015) restrict the accretion of the angrites parent body (APB) to the first 0.25 ± 0.15 Ma of CAI formation. The differentiation process with development of a metallic core seems to have been an early event, as estimated from ^{182}Hf–^{182}W systematics (Kleine et al., 2012). The efficiency of such separation process seems to have been variable to account for the highly variable (from 0.2 to $0.00001 \times$ CI) siderophile element contents of angrites (Riches et al., 2012).

The mineralogical composition of angrites is unusual. All phase assemblages are usually out of equilibrium. Fe-Al-Ti-rich augite coexists with anorthite, Mg-rich olivine, Ca-Fe-rich olivine, kirschsteinite, a variety of oxides, phosphates, sulfides and some Ni, Fe metal (e.g., Prinz et al., 1977; Mittlefehldt et al., 2002; Kurat et al., 2004; Varela et al., 2015). Textural studies indicate that olivine, plagioclase and pyroxene crystallized simultaneously during a significant part of angrites formation history (e.g., Mikouchi et al.,1996; Mittlefehldt et al., 2002; Floss et al., 2003). Based on their textures and cooling rates, angrites have been divided into two subgroups: coarse-grained ("slowly-cooled" plutonic angrites, e.g., Angra dos Reis, LEW 86010) and fine-grained ("quenched" volcanic angrites, e.g., Asuka 881371, D'Orbigny) (see Keil, 2012 and references therein). Based on the U-Pb, Hf-W and Mn-Cr chronometers, the two subgroups correlate with two different periods of igneous activity separated by ~5–6 Ma, (e.g., Glavin et al., 2004; Amelin, 2008; Bouvier et al., 2011).

The angrite D'Orbigny is exceptional among this small group of meteorites in several respects. Its shape, somewhat like a loaf of bread, has a back and front shields characterized by a compact lithology with the space in between these shields filled by a very porous lithology (Fig. 1A). Such a shape requires directional growth in free space (e.g., Kurat et al., 2004). The compact shield rock has a medium-grained micro-gabbroic texture with dispersed druses, with perfectly crystallized augites of prismatic habit and hollow spherical shells (Fig. 1B). It shows a gradual transition into the porous lithology in which the grain-size, pore-size and abundances of druses and hollow spheres increase (Kurat et al., 2004). The textural studies of the dense part of D'Orbigny give evidence for co-crystallization of olivine + anorthite and olivine + anorthite + augite (Fig. 1C). However, the porous part of D'Orbigny consists mainly of a fluffy, highly porous aggregate of anorthite-olivine intergrowths with the pore space being totally or partly filled by augite (e.g. Kurat et al., 2004). Hence, D'Orbigny differs from other angrites that are considered to represent crystallized liquids (Asuka 881371, LEW 87051) or metasomatic granoblastic rocks (LEW 86010, Angra dos Reis).

The angrite D'Orbigny is also unusual in that it contains abundant glass (Varela et al., 2003). These glasses have been interpreted as due to a volcanic origin of the rock and therefore a supporting evidence for magmatism on the APB (e.g., Mittlefehldt et al., 2002). However, one of the most unexpected results in D'Orbigny glasses is the presence of trapped noble gases of solar-like composition (Busemann et al., 2006). The cosmic-ray exposure age of D'Orbigny is striking. While the age of the bulk is 11.7 ± 0.7 Ma, that of the glass is 1.6 ± 0.6 Ma, suggesting a pre-exposure of the bulk relative to the glass (Busemann et al., 2006). However, the Mn-Cr age indicates that glasses in D'Orbigny were formed contemporaneously with the olivine, pyroxene, chromite and bulk rock (Glavin et al., 2004); a clear evidence that glasses co-exist with all other phases and were not introduced into D'Orbigny later.

These glasses give the most compelling evidence against an igneous origin of D'Orbigny. The compositional features of all types of glasses (e.g., primary glass inclusions in olivines, glass patches, glass spheres, etc.): including (1) with abundances of refractory elements (e.g., Al, Ti, Ca) at $10 \times$ CI, (2) with CaO/TiO_2 and FeO/MnO ratios being approximately chondritic and (3) with significant contents of C and N in glasses of glass inclusions, point towards a primitive origin (Varela et al., 2003). In addition, in spite of having different major element compositions, all glasses show the same trace element pattern. That is, glasses filling open spaces commonly in contact with several phases and also open to the environment (e.g., glass spheres and glass patches), have trace element abundances indistinguishable from those trapped as primary glass inclusions in olivine (e.g., in contact only with olivine). This particular chemical feature cannot be reconciled with an igneous system. Therefore, the partial melting hypothesis of a chondritic source for angrite petrogenesis might be excluded, as no elemental fractionation related to compatibility can be detected. The trace element patterns of glasses are characterized by being strongly depleted in volatile lithophile elements, with unfractionated relative abundances of refractory lithophile elements, and point towards vapor fractionation (Varela et al., 2003). This suggests that the process involved in glass formation was governed by cosmochemical—rather than a geochemical—fractionation.

Also, the original angrite assemblage appears to have been compositionally modified by metasomatic alterations with subsolidus processing after formation (Kurat et al., 2004) or by late anhydrous migratory metasomatic fluids (Irving et al., 2008) (Fig. 1D).

In addition to many of the unusual features of this rock, D'Orbigny is characterized by having large olivine megacrysts similar to those present in other angrites: LEW 87051, Asuka 881371, and NWA 1670 (Mikouchi et al., 2011). However, the rock is unique in having large polycrystalline olivinites showing a very complex texture characterized by having large angular or round olivine fragments (0.5–1 mm) surrounded by a very fine-grained olivine groundmas as explained, in detail, below.

Previously we were able to investigate the complete mass (16550 grs) of this angrite in three dimensions (e.g., Kurat et al., 2004) and collected several of these olivinites. We report here a detailed study on five olivinites that will provide some insights into one of the earliest constituents of this rock.

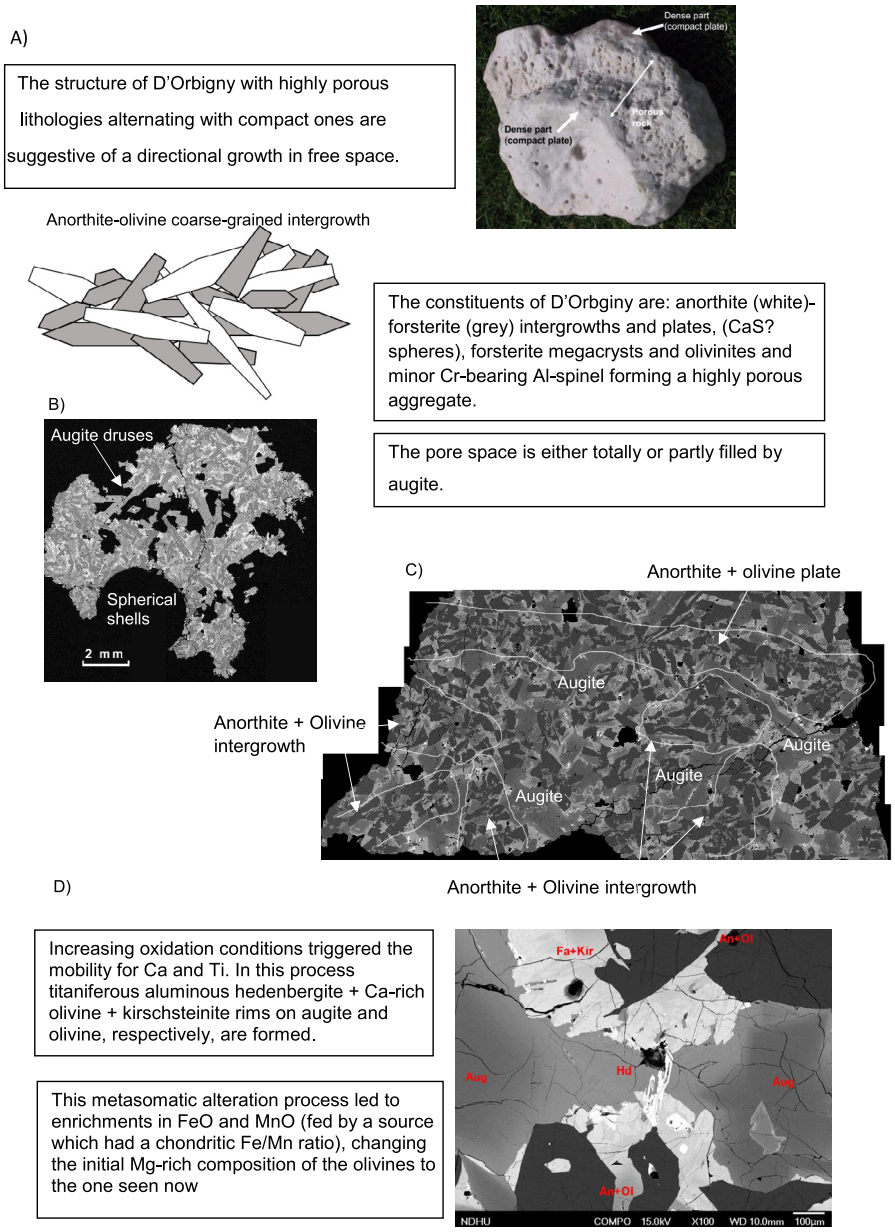

Fig. 1. Cartoon figure describing the history of D'Orbigny. (A) A plaster copy of D'Orbigny showing the compact lithology of the back and front shields with the space in between these shields filled by a very porous lithology. Also shown is a sketch of an anorthite-olivine intergrowth. (B) Back-scattered electron (BSE) image of the porous lithology showing augite druses and a hollow spherical shell. (C) Combined BSE montage showing the dense lithology with an anorthite-olivine plate and anorthite-olivine intergrowths. The pore space is either totally or partly filled by augite. Length of the image: 2 cm. (D) BSE image showing the titaniferous aluminous hedenbergite rim (Hd) and the Ca-rich olivine + kirschsteinite rims (Fa + Kir) on augite and olivine. Aug: augite, An + Ol: anorthite + olivine.

Keil (2012) previously noted in a comprehensive review of angrites that many important data have been published in the form of abstracts, therefore this paper, which includes our preliminary reports on D'Orbigny olivinites (Abdu et al., 2011; Hwang et al., 2012), is a contribution intended to rectify this problem.

2. ANALYTICAL TECHNIQUES AND SAMPLES

Five olivinites were analyzed in polished thick sections (Olivinite 1 - Olivinite 5, samples from ICATE: **I**nstituto de **C**iencias **A**stronomicas de la **T**ierra y del **E**spacio). Two additional olivinites were analyzed by Transmission Electron Microscopy (TEM), Fourier transform infrared (FTIR) and micro-Raman and Mössbauer spectroscopy. Samples were studied with a petrographic microscope and a JEOL JSM-6610 scanning electron microscope (NHM Vienna) operated at a sample current of ~1 nA and an acceleration voltage of 15 kV. Major element chemical compositions were obtained with an ARL-SEMQ (ICATE) and a JEOL JXA-8530F FE (NHM Vienna) electron microprobes. Electron microprobe analyses (EMPA) were

performed using a 15 kV acceleration potential and ~15 nA sample current.

Micro-Raman spectroscopy measurements were done using a LabRAM ARAMIS confocal microscope, Horiba Jobin Yvon (University of Manitoba, Canada). An 100× objective microscope was used to focus the laser beam (532 nm excitation line) on the sample to a size of ~1 μm. The wave number was calibrated using the 520.7 cm^{-1} line of Si metal.

FTIR spectra over the range (4000–400 cm^{-1}) were collected on KBr sample pellets using a Bruker Tensor 27 FTIR spectrometer (University of Manitoba, Canada). Transmission Mössbauer spectra were acquired at room temperature (RT) using a ^{57}Co(Rh) point source (University of Manitoba, Canada).

For TEM studies the polished thin section was studied by optical microscopy and analytical scanning electron microscopy (FE SEM) to find the areas of interest. TEM samples from such areas were then prepared by the FIB (Focused Ion Beam) technique (National Sun Yet-sen University, Taiwan) for selected area electron diffraction (SAED) using a JEOL 3010 AEM (National Dong Hwa University, Taiwan).

3. RESULTS

3.1. Petrography

Olivine is present throughout the rock and is usually intimately associated with anorthite, forming complex intergrowths. Large olivine crystals are more common in the porous part than in the rest of D'Orbigny. There are two varieties:

1. Large green and honey coloured crystals (olivine megacrysts), which are clear and transparent and have tracks of secondary fluid/mineral inclusions, commonly containing sulfides.
2. Large polycrystalline olivinites.

3.1.1. Olivinites (polycrystalline olivine) consist of large, clear, green olivine grains of up to 8 mm in diameter (Fig. 2)

Their shapes are very complex ranging from thin shards through irregular fragments to blocky fragments. The polycrystalline olivinites are intimately intergrown with the host rock and are mostly accompanied by anorthite-olivine intergrowths.

Olivinites have a very complex texture characterized by two different domains: (1) large angular or round olivine fragments (0.5–1 mm) surrounded by (2) a very fine-grained olivine groundmass (Fig. 2B and C). In addition, three olivinites show spinel fragments and veins.

The Fourier-transform infrared (FTIR) spectra of the olivinite show that no structural OH bands are present in the OH-stretching region (3800–3000 cm^{-1}). The room temperature (RT) Mössbauer spectrum of the olivinite consists of two asymmetric absorption peaks, resulting from the overlap of two quadrupole doublets because of the presence of Fe^{2+}in the M1 and M2 octahedral sites (Fig. 3). The spectrum shows an additional weak doublet (CS = 0.35 mm/s, QS = 0.30 mm/s, Area = 2%) which is attributed to Fe^{3+} (Fig. 3).

3.1.1.1. Large angular or round olivine fragment. Under optical microscopy the large olivine fragments (Fig. 2, B2 arrowed) are polycrystalline with a small (20 μm) average grain size that is 5 to 10 times larger than that of the fine-grained groundmass olivine (Fig. 2B and C). The small crystals forming the fragments are characterized by a similar extinction angle (Fig. 2C), indicating that their crystal axes are oriented similarly in space. Therefore, fragments could represent recrystallized sub-grains of a former single forsterite crystal as supported by the well-preserved crystal faces (arrows in Fig. 2B2). Most subgrains in the fragment are inclusion-free except for the presence of bands of very abundant multiple-phase inclusions, consisting of sulfide (FeSx) + Fe-Ni metal + bubble, winding through the fragment domains (Fig. 4A and B).

TEM images from FIB sections cut across the recrystallized grains in the olivine fragment (Fig. 2C2) show great differences in defect microstructures across the grain boundaries of the recrystallized grain (Fig. 5A). The olivine fragment shows abundant defect microstructures (Fig. 5A) with some sub-grain boundaries decorated by dislocations and several bubbles (Fig. 5B and C). In contrast the recrystallized grain is dislocation-free (Fig. 5A). The fragments show abundant ribbon-like trails of multiphase (FeS_x + -Fe-Ni metal + bubbles) inclusions.

3.1.1.2. Fine-grained olivine groundmass. On the other hand, the olivine in the olivinite groundmass has a fine-grained texture (Fig. 2C3) and heterogeneous distribution of primary inclusions. Many grains in the olivinites groundmass contain submicrometer-size, rounded to ellipsoid inclusions/voids located at the cores and varying in size between ~0.1 and 1 μm (Figs. 4C–D and 6). The inclusion/void abundance varies among grains, with the larger ones having the higher inclusion/void density (Fig. 4D). Inclusion-free rims of 5–10 μm in thickness are always present in these grains, and grains <10 μm in diameter are generally inclusion-free (Fig. 4C and D). Based on the SEM-EDX analyses on these inclusions, the void interiors appear to be clean (mostly empty) except for the presence of one facetted precipitate on the void wall (arrows in Fig. 6C1). An EDX spectra of these tiny crystals indicate that they are Cr-spinels (Cr-Spl) with Cr# (Cr/Cr + Al) = ~0.3. The size of these Cr-spl precipitates seems to be directly proportional to the volume of each ellipsoidal void. Iron sulfides are not included at the grain cores, but instead sit at the grain boundaries, especially at the triple-junctions, within the olivinite groundmass (Fig. 4C and D, arrowed). The SEM-EDX analyses (Fig. 6) show that, besides sulfide, Al-Si-Ca phases (atomic ratio ~2:~2:~1 indicative of anorthite) (Fig. 6A1-2), Fe-poor augites (Fig. 6A1–B2) and Al-spinels with Cr# = 0.1 (Fig. 6B) are always present on the grain boundaries.

TEM images (Fig. 6C1–C2) show several, partially $\{100\}_{Fo}$ facetted, ellipsoidal voids of various sizes in association with dislocations within the small olivine from the

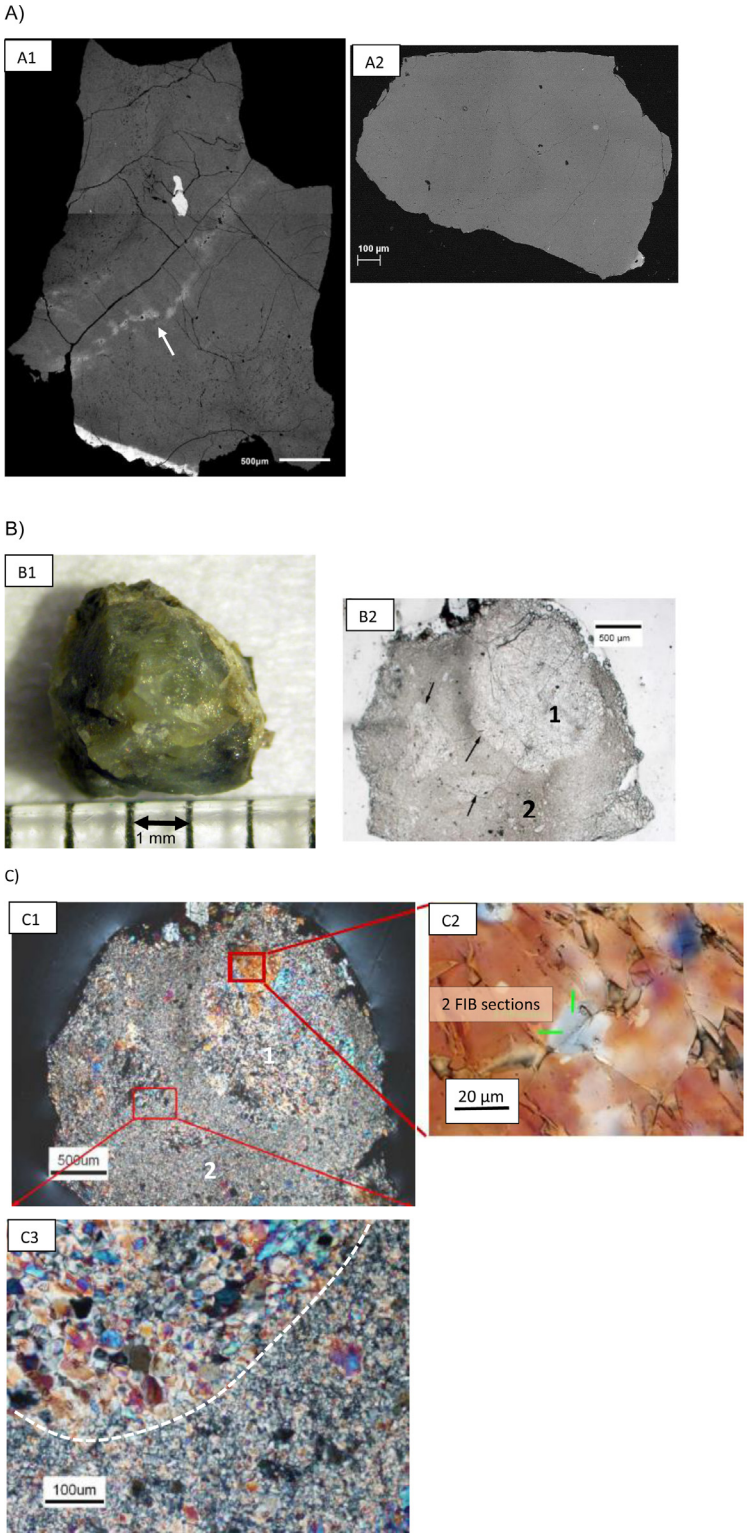

Fig. 2. (A1–A2): Back-scattered electron (BSE) image of olivinite 1 and 4, respectively. White arrow in (A1) points a secondary vein. (B1) Hand sample and thin section (B2) of the olivinite used for TEM studies. (B2) shows the two different domains that characterize olivinites: the angular or round olivine fragments (0.5–1 mm) (labelled: 1), surrounded by very fine-grained olivine groundmass (labelled: 2). Black arrows point to large angular or round olivine fragments. (C1) Optical polarized micrograph under crossed polarizers showing both domains: 1 and 2. (C2) showing the place in which two FIB sectioning were performed (green lines), cutting across the recrystallized grains in the olivine fragment. (C3) showing detail of the texture in a small fragment and the fine-grained groundmass. The boundary of the two separate areas is indicated by a white dashed line. (For interpretation of the references to colour in this figure legend, the reader is referred to the web version of this article.)

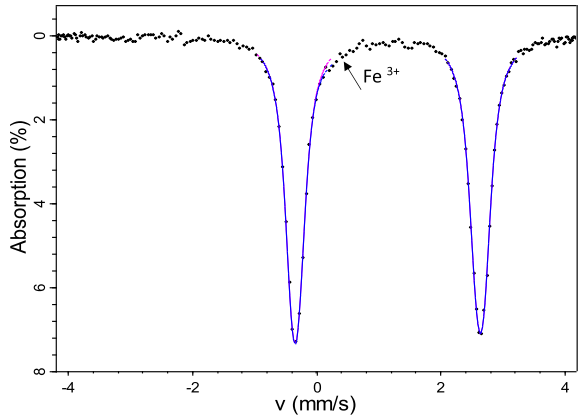

Fig. 3. Room temperature (RT) Mössbauer spectra of the olivinite showing the two asymmetric absorption peaks. Note the additional weak doublet (CS = 0.35 mm/s, QS = 0.30 mm/s, Area = 2%) which is attributed to Fe^{3+}.

groundmass. Except for the deposition of Ga from FIB operation for the larger, open voids (Fig. 6C2), the interior of each void appears to be clean with the presence of only a single euhedral Cr-Spl crystal epitaxially embedded/attached to one of the olivine {100} walls (Fig. 6C1–C3). The crystallographic orientation relationships (COR) between Cr-spl and olivine are: $\{111\}_{Sp}//\{100\}_{Fo}$, $\langle 110\rangle_{Sp}//\langle 001\rangle_{Fo}$.

The fact that the voids (primary glass inclusions?) have ellipsoidal shapes that are controlled by the crystal structure supports a primary origin. Similarly, the Cr-spl might have been formed from a precursor medium (e.g., as a pre-existing crystal) that was trapped during formation of the now empty inclusions. The COR between Fo and Cr-spl is $(111)_{Sp}//(100)_{Fo}$, $[1\bar{1}0]_{Sp}//[001]_{Fo}$. Besides the abundant Cr-spl-bearing voids the Si-Al-Ca glass inclusions with co-existing Cr-spl + Fe-Ni globule were also occasionally observed in TEM analyses (Fig. 6C4–C6).

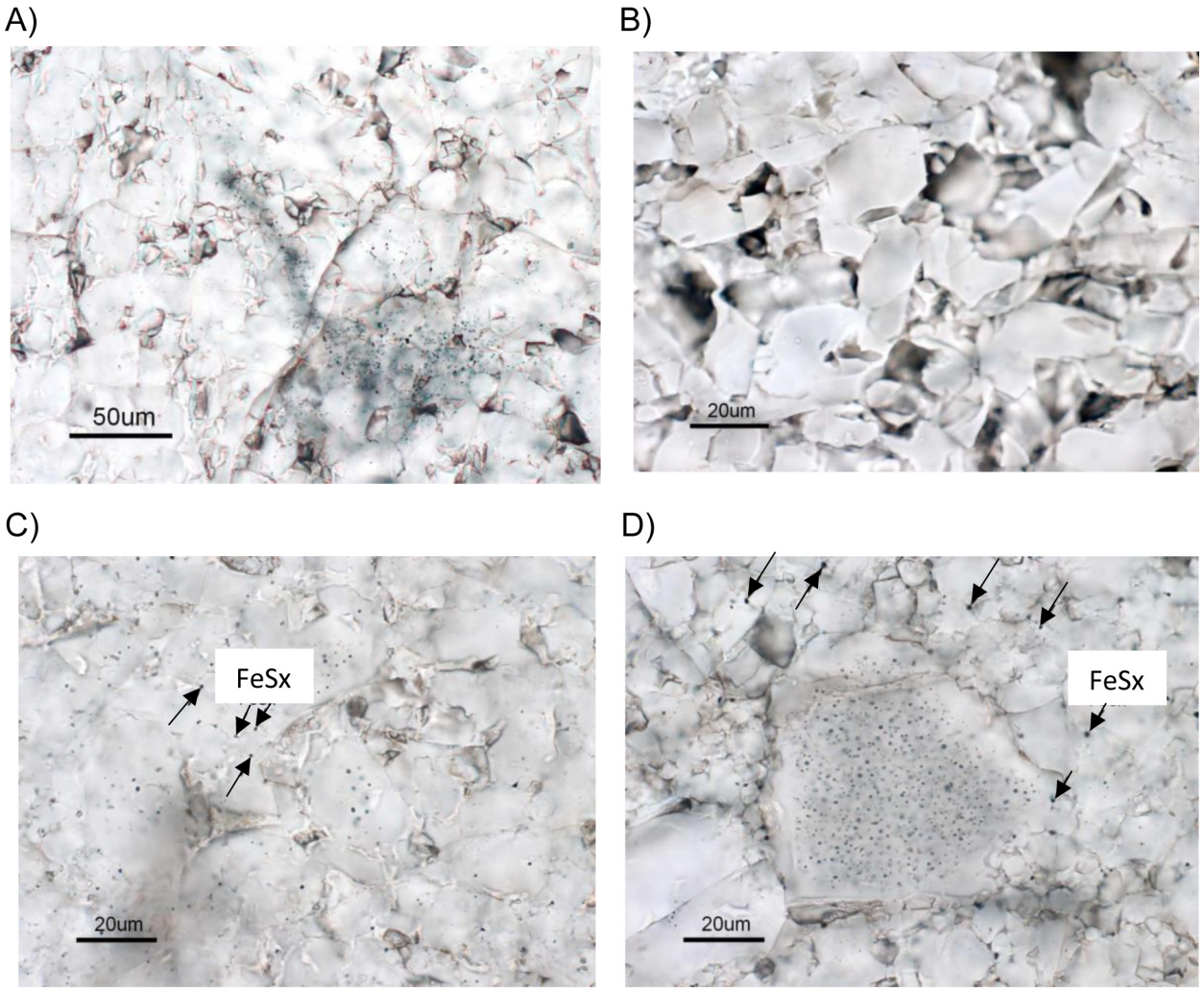

Fig. 4. Optical polarized micrographs under open polarizer showing the fine-grained olivines from the groundmass: (A) Subgrains in the fragment that are inclusion free except for the presence of bands of very abundant dark inclusions. (B) Inclusion-free fine-grained texture of the olivine groundmass. (C) Sulfides (arrows) sitting at the grain boundaries, especially at the triple-junctions, within the groundmass. (D) Large olivine grains having cores with high inclusion/void density and inclusion-free rims.

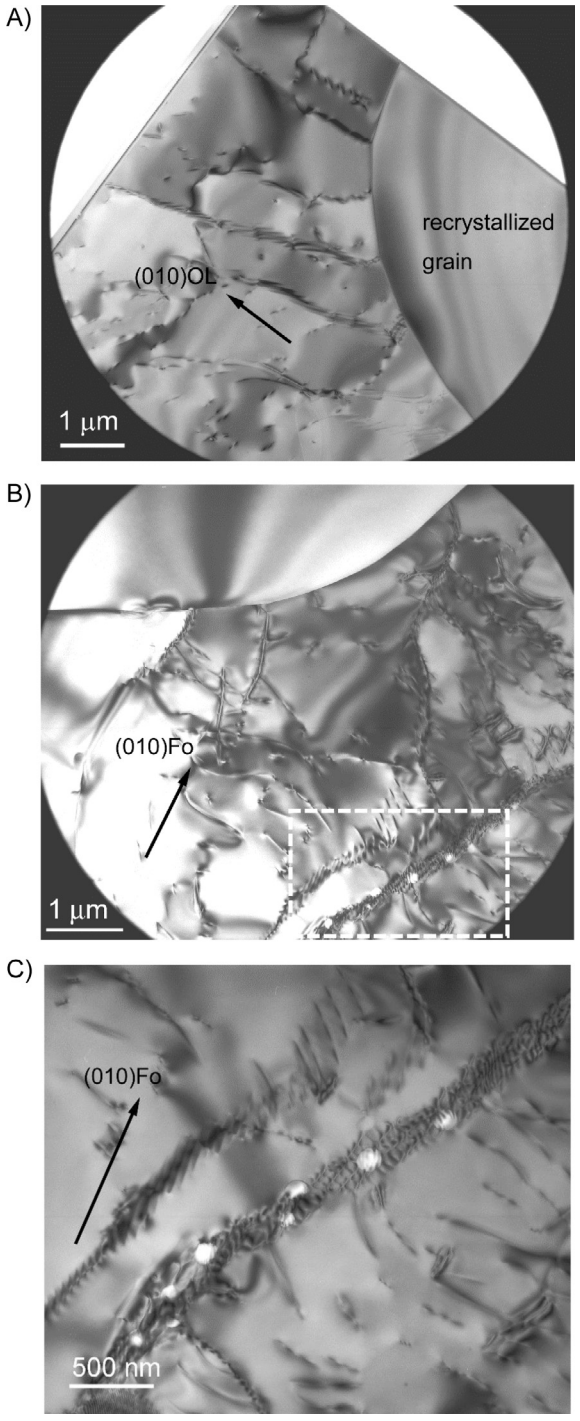

Fig. 5. TEM images showing: (A) Abundant defect microstructures in the olivine fragment across the grain boundaries of the recrystallized grain Location of the FIB sections are shown in Fig. 1C2). In contrast the recrystallized grain is dislocation-free. (B and C) Sub-grains boundaries decorated by dislocations and several bubbles.

3.1.1.3. Spinel fragments and veins. Besides the aforementioned microstructural features, three of the studied olivinites show spinel fragments that vary in size from ≈400 μm to 50 μm with a compact or porous texture. Both tex-

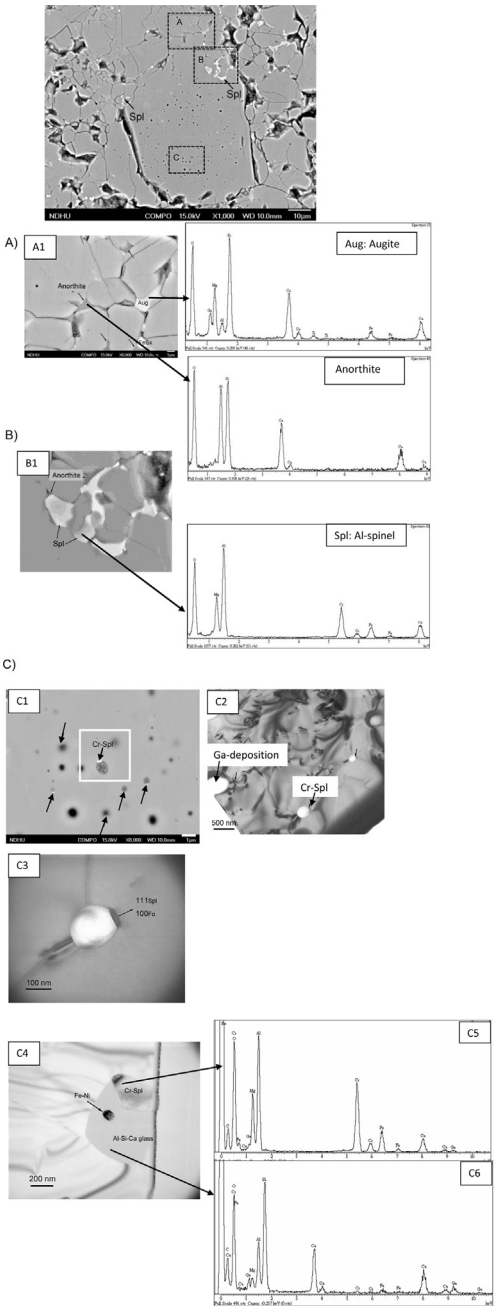

Fig. 6. Back-scattered electron (BSE) images showing the heterogeneous distribution of inclusions with inclusion-rich core and inclusion-free rims in coarse and fine-grained olivines from the groundmass (similar to Fig. 4D). Three rectangular areas (A, B and C) are indicated. Area (A-B) BSE image of phases in between olivine grains. The SEM-EDX analyses show the presence of anorthite, Augite: Fe-poor augite and Spl: Al-spinel (B). (C1) BSE image of olivine groundmass showing ellipsoid voids of variable sizes at grain cores. Note that only a single Cr-Spinel crystal is attach to each void. (C2) TEM image of olivine groundmass show abundant dislocations and ellipsoid voids with variable sizes. (C3) Detail of the ellipsoidal void, facetted by $(1\,0\,0)_{Fo}$ with an euhedral Cr-spinel crystal partially embedded within olivine walls. (C4) One void is a Si-Al-Ca glass inclusion with co-existing Cr-spinel + Fe-Ni globule. The SEM-EDX analysis shows the Cr-spinel (C5) and the Si-Al-Ca glass (C6).

tures can be present in a single fragment (Fig. 7A, C). Another feature of the olivinites is the presence of secondary /pseudo-secondary veins (see arrows in Fig. 2A) up to 1 mm in length, full of subhedral to euhedral crystals with variable sizes (20–40 μm in length) of spinel, anorthite, clinopyroxene together with glass.

3.2. Mineral Chemistry

3.2.1. Olivine

Olivine grains from the five studied olivinites have a chemical composition range of $Fa_{8.9–10.4}$ and are CaO-poor ($Lrn_{0.3–0.5}$) (Table 1). The mg# value (mg#: 90) estimated from Raman spectroscopy, using the ω (= κ1 – κ2) – mg# (mg# = −0.17744–0.050049 ω + 0.0026479 ω2) and those calculated from EMPA are in close agreement (Abdu et al., 2011).

3.2.2. Spinel fragments

These fragments are mainly chemically homogeneous with Al_2O_3 contents varying from 32.5 to 38.4 wt% and Cr_2O_3 contents from 33.1 to 36.5 wt% (Table 2, Fig. 8). Reactions rims were detected only in one fragment in olivinite 2 (inset Fig. 7B) with Al_2O_3 contents ~43.6 wt% and Cr_2O_3 contents ~21.2 wt% (Fig. 8). No chemical variation could be observed between spinels with a compact or porous texture. Only one such fragment is chemically zoned (Fig. 7C, Olivinite 4, Table 2) with higher Al_2O_3 (54–60 wt%) and lower Cr_2O_3 (6.6–7.8 wt%) contents, as compared to those fragments from olivinites 1 and 2 (Table 2) and to the spinel grains from the groundmass of D'Orbigny (Fig. 8).

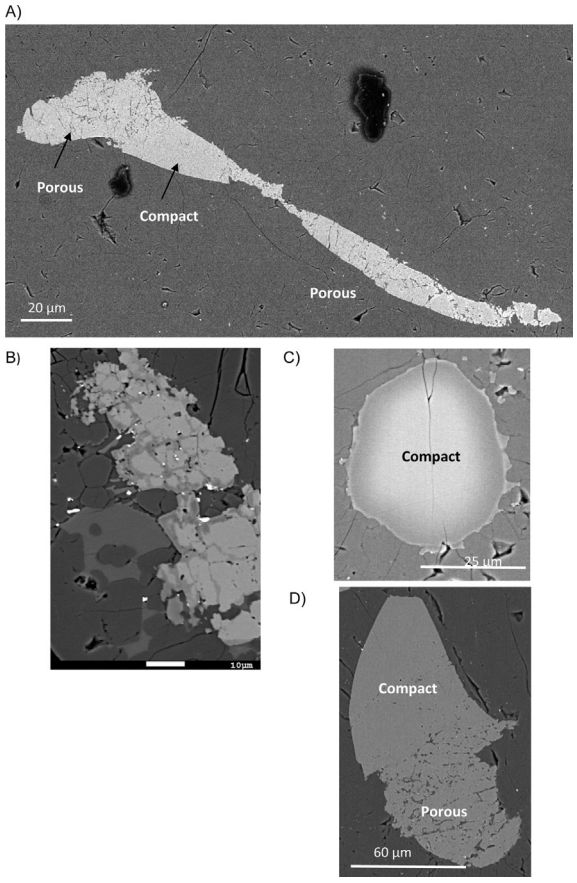

Fig. 7. (A-B-C) Back-scattered electron (BSE) images of spinel fragments present in olivinites. Note the compact and porous texture that characterized all these fragments as well as the reaction rim in one of the fragments in olivinite 2 (B) and the irregular rim in the spinel fragment of olivinite 4 (D).

3.2.3. Veins

The phases forming part of the veins are: pure anorthite, clinopyroxene ($Wo_{48.9}$ $En_{40.3}$ $Fs_{10.9}$) and mesostasis glass (SiO_2: 49 wt%, CaO: 22 wt%, Al_2O_3: 8 wt%, MgO: 12 wt%, FeO: 7 wt% and TiO_2: 2 wt%) with a $Diop_{96.3}$ $Plag_{21.7}$ Ol_5 normative composition (Table 3). Spinel in veins ($Sp_{0.72}$ $Ch_{0.17}$ - $Sp_{0.74}$ $Ch_{0.16}$, Table 3) show that their increment in Al_2O_3 contents is coupled with a decrease in their Cr_2O_3 contents. They fill the compositional gap between the Cr-rich spinel fragments in olivinites and the Cr-bearing Al-rich spinel present in D'Orbigny (Fig. 8). A few spinel grains are zoned, with Cr-rich cores and Al-rich rims.

3.2.4. Spinel in glasses

The TEM-EDX data of the tiny spinel crystals that form part of the ellipsoidal voids filled with a Ca-Al-rich glass within olivine grains (Fig. 6C) and the SEM-EDX data of those present at grain boundaries (Fig. 6B) show a similar compositional variation. Spinel trapped in primary glass inclusions are richer in Cr_2O_3 (~Al_2O_3: 42 wt%, MgO: 18 wt%, Cr_2O_3: 30 wt%, FeO: 10 wt%) compared to that present at grain boundaries (~Al_2O_3: 53 wt%, MgO: 19 wt%, Cr_2O_3: 19 wt%, FeO: 9 wt%) (Fig. 8).

4. DISCUSSION

4.1. Is D'Orbigny an exception among all other angrites?

The prevailing view that angrites are igneous rocks of basaltic composition (e.g., Mittlefehldt and Lindstrom, 1990; Longhi, 1999; Mittlefehldt et al., 2002; Floss et al., 2003) faces two unsolved problems. First, creating a liquid of such unusual composition (e.g., the source of angritic liquids remains unknown) and second, crystallizing a rock from such a liquid with the observed mineralogy and mineral composition of angrites. Although D'Orbigny is the most studied of the recently found angrites, this particular rock symbolizes "a third problem" to be solved in order to advance in the comprehension of angrites. It is difficult to reconcile an igneous origin of this rock with the particular structure and a mushroom-like shape that requires directional growth in free space with alternating texturally different layers (Fig. 1), or with the different types of glasses that show no evidences of geochemical fractionation (Varela et al., 2003). Although it is classified as a fine-grained "quenched" angrite (see Keil 2012 and references there in) D'Orbigny has druses that are omnipresent in the porous portion, with druse crystals –perfectly euhedral augites millimeters in size - protruding into free space, resembling the terrestrial druses formed by a pneumatolytic process (Fig. 1B). A detailed study of all constituents of

Table 1
Representative EMP analysis of olivine in olivinites.

	Olivinite 1		Olivinite 2		Olivinite 3		Olivinite 4		Olivinite 5	
	ave	std	ave	*std*	ave	*std*	ave	*std*	ave	*std*
n	*8*		*12*		*9*		*10*		*11*	
SiO_2	40.6	0.9	39.1	*0.7*	40.6	*0.4*	39.5	*0.3*	40.1	*0.4*
TiO_2	0.03	0.03	0.02	*0.05*	0.01	*0.03*	0.02	*0.02*	0.02	*0.01*
Al_2O_3	0.09	0.08	0.07	*0.01*	0.35	*0.03*	0.15	*0.05*	0.09	*0.02*
Cr_2O_3	0.21	0.05	0.17	*0.03*	0.2	*0.02*	0.24	*0.06*	0.25	*0.03*
FeO	8.8	0.5	10.2	*0.8*	9.3	*0.9*	10.3	*0.6*	9.6	*0.3*
MnO	0.06	0.02	0.08	*0.03*	0.1	*0.03*	0.11	*0.05*	0.11	*0.03*
MgO	50.4	0.5	49.8	*0.5*	49.7	*0.8*	49.6	*0.9*	49.7	*0.4*
CaO	0.24	0.04	0.4	*0.05*	0.29	*0.06*	0.33	*0.05*	0.29	*0.05*
Total	100.4		99.8		100.6		100.3		100.2	
Fo	90.7		89.2		90.1		89.1		89.8	
Fa	8.9		10.2		9.5		10.4		9.7	
Ca-Ol	0.3		0.5		0.4		0.4		0.4	

n: Number of analyzes performed.

Table 2
Representative EMP analysis of spinel in olivinites.

	Olivinite 1			Olivinite 2					Olivinite 4	
	Sp 1	Sp 2	Sp 3	Sp 1		Sp 2		Sp 3	Sp 1	
		ave	ave	ave	*std*	ave	*std*	ave *std*	ave	std
n	*1*	*2*	*2*	*20*		*10*		*4*	*15*	
SiO_2	0.23	0.51	0.51	0.5	*0.2*	0.44	*0.1*	0.7 *0.2*	2.6	0.9
TiO_2	0.32	0.16	0.35	0.32	*0.03*	0.31	*0.01*	0.33 *0.01*	0.26	0.04
Al_2O_3	32.5	33.5	34	37.9	*0.5*	38.4	*0.3*	37.2 *0.8*	57.1	1.4
Cr_2O_3	35.9	36.5	36.6	33.9	*0.8*	34.2	*0.6*	33.1 *0.4*	7.1	0.3
FeO	10.9	10.7	9.7	11.5	*0.8*	10	*0.6*	11.8 *0.6*	17.8	4
MnO	0.02	0.02	0.06	0.02	*0.01*	0.02	*0.01*	0.07 *0.02*	0.08	0.03
MgO	18.8	18.5	19.4	16.2	*0.8*	17.3	*0.4*	15.8 *0.7*	16	3
CaO	0.02	0.03	0.02	0.03	*0.01*	0.03	*0.01*	0.02 *0.01*	0.03	0.01
Total	98.7	99.9	100.6	100.4		100.7		99.0	101.0	
mg-no	0.83	0.79	0.81	0.68		0.72		0.68	0.64	
cr-no	0.43	0.42	0.38	0.38		0.37		0.37	0.08	
Spinel	0.60	0.79	0.82	0.69		0.72		0.68	0.64	
Hercynite	-0.05	-0.23	-0.25	0.05		0.08		0.05	0.26	
Magnetite	0.03	0.02	0.02	0.02		0.02		0.02	0.02	
Chromite	0.38	0.41	0.41	0.38		0.38		0.38	0.08	
Ulvöspinel	0.01	0.00	0.01	0.01		0.01		0.01	0.01	

n: Number of analyzes performed.

D'Orbigny coupled with a trace element study of all phases, occurring either in the porous and dense portions of the rock, led Kurat et al. (2004) and Varela et al. (2003, 2005) to propose an alternative model for formation of this angrite at odds with the igneous model. They suggested that D'Orbigny formed in the solar nebula under changing redox conditions in a manner more akin to that of formation of chondritic constituents (e.g., CAIs) rather than to a planetary differentiated rock.

D'Orbigny appears to be unique, and is a heterogeneous mixture of some constituents that were able to record the large variety of conditions prevailing during formation of angrites. Vestiges of the early reducing conditions may be found in one of the oldest constituents of D'Orbingy: the olivine megacrysts and olivinites.

4.2. Are Mg-rich olivine rare phases to angrites?

Olivinites together with olivine megacrysts are the most magnesian phases encountered in angrites (e.g., Prinz and Weisberg, 1995; Mittlefehldt et al., 2002; Kurat et al., 2004; Mikouchi et al., 2011). Such a Mg-rich composition (mg# 90) is far away from that of possible precipitates from angrite parent melts and therefore olivinites, as well as olivine megacrysts, were considered as "xenocrysts" (e.g., Prinz et al., 1990; Mittlefehldt et al., 2002; Mikouchi et al., 2011). However, the study of the whole angrite D'Orbigny in three dimensions indicate that olivinites and olivine megacrysts would be one of the first building blocks of this rock. Recently, a study of new angrites NWA 8535 (Agee et al., 2015; Santos et al., 2016) showed that this rock

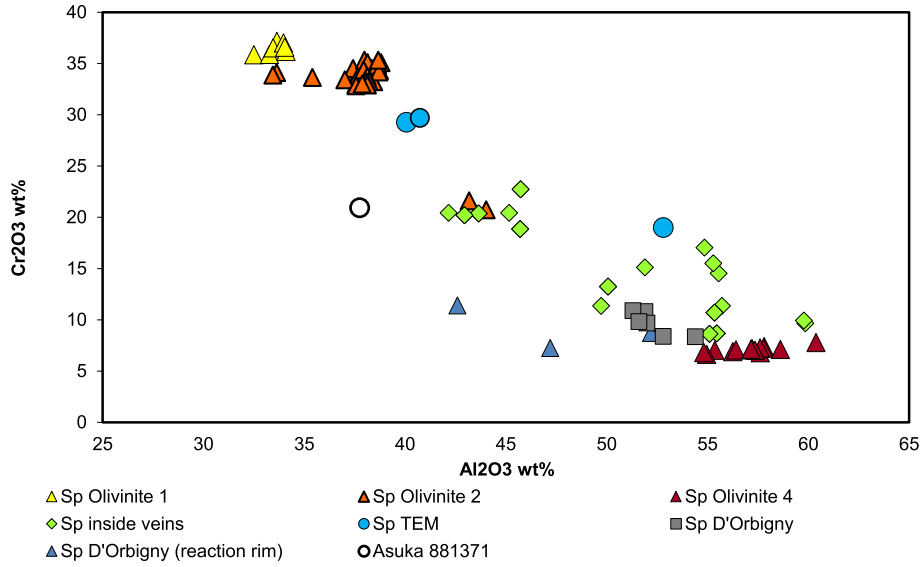

Fig. 8. Cr_2O_3 vs Al_2O_3 diagram of all types of spinels encountered in olivinites of D'Orbigny. Spinel from angrite Asuka 881371 is given for comparison.

Table 3
Representative EMP analysis of minerals inside veins olivine in olivinites.

	Olivinite 1						Olivinite 2					
	Spinel		Anorthite		Olivine		Spinel		Anorthite		Clinopyroxene	
	ave	*std*	ave	*std*	ave	*std*	ave	*std*	ave	*std*	ave	*std*
n	*10*		*4*		*4*		*16*		*7*		*16*	
SiO_2	0.31	*0.05*	43.4	*0.2*	38.8	*0.6*	0.28	*0.08*	43.5	*0.4*	46.1	*0.9*
TiO_2	0.47	*0.2*	0.03	*0.01*	0.09	*0.03*	0.4	*0.03*	0.02	*0.01*	2.28	*0.3*
Al_2O_3	49.5	*5*	34.2	*0.3*	0.03	*0.01*	51.5	*6*	34.1	*0.4*	7.6	*1.3*
Cr_2O_3	15.5	*5*	0.03	*0.01*	0.1	*0.03*	14.8	*4.7*	0.04	*0.01*	0.51	*0.03*
FeO	14.8	*1.5*	0.93	*0.02*	16.8	*0.6*	13.3	*1.4*	1.05	*0.05*	6.5	*1*
MnO	0.08	*0.02*	0.03	*0.01*	0.15	*0.02*	0.05	*0.01*	0.02	*0.01*	0.07	*0.03*
MgO	17.6	*1*	0.43	*0.05*	44.1	*0.4*	18.5	*1.5*	0.89	*0.05*	13.5	*1*
CaO			20.6	*0.01*	0.64	*0.05*			20	*0.3*	22.8	*0.6*
Total	98.3		99.7				98.8		99.6		99.4	
Fo					81.6							
Fa					17.4							
Ca-Ol					0.9							
Mg-No	*0.71*						0.74					
Cr-No	*0.17*						0.16					
Spinel	*0.72*						0.74					
Hercynite	*0.08*						0.07					
Magnetite	*0.02*						0.02					
Chromite	*0.17*						0.16					
Ulvöspinel	*0.01*						0.01					
An			100						100			
Ab			0						0			
Or			0						0			
Wo											48.9	
En											40.3	
Fs											10.9	

n: Number of analyzes performed.

is a dunite (90–95% olivine) composed of Mg-rich olivines with a range of magnesium numbers (mg#) from 70 to 88. In NWA 8535 olivines are zoned with higher values in the core ($Fo_{84.5}$ $Fa_{15.4}$ $Lrn_{0.2}$) compared to those in the rim ($Fo_{75.3}$ $Fa_{23.8}$ Lrn_1) (Santos et al., 2016). The presence of zoned olivines suggests rapid cooling and therefore NWA 8535 could be more related to the so-called volcanic angrites (Agee et al., 2015). They noted that the composition of the proposed "xenocrystic" olivines in the volcanic angrites Asuka 881371 and D'Orbigny overlap with those

of the olivines in NWA 8535. Therefore, Mg-rich olivines are not genetically unrelated to angrites but indeed form one of their constituent phases either, as a small part of the rock (e.g., Asuka 881371 and D'Orbigny) or as the majority of it (NWA 8535).

Our detailed study of olivinites indicates that the fayalite content of about 35 mol.% that characterized olivine in the groundmass of D'Orbigny – as well as other angrites (Keil, 2012)-does not correspond to its original composition but may be the result of a late process that affected these rocks. Therefore, olivinites may indicate the pristine more reducing conditions –akin to those prevailing during NWA 8535 formation- that are preserved in some other angrites.

4.3. The messages recorded in olivinites

Olivinites are characterized by having a peculiar texture, spinel fragments and phase compositions that provide information related with both, early formation and later alteration processes. This will be discussed in detail in the following.

4.3.1. The texture

The nature of the very fine-grained polycrystalline olivinite is enigmatic. This texture could be a secondary breakdown product of former well-crystallized olivines. Mikouchi and McKay (2001) suggested that similar textures in olivine megacrysts could be the result of shock. However, as D'Orbigny has no indications of shock (e.g., Mittlefehldt et al., 2002), this texture could be the result of a thermal event. Our TEM studies show great differences in defect microstructures across the grain boundaries of the recrystallized grains (Figs. 2C2 and 5A). Apparently, the recrystallization process converted some of the defect/dislocation domains into defect/dislocation-free domains (Fig. 5A). TEM images show that grain boundaries are decorated by several diffusion-induced bubbles (Fig. 5B and C). Although these bubbles are similar to the ellipsoidal voids observed in the olivines of the fine-grained groundmass (Fig. 6), no Cr-spinel crystals are attached to them. The existence of abundant defect microstructures in the polycrystalline olivine fragments of olivinites indicates that the fine-grained texture could be a primary feature. In some respects, they resemble the fine-grained texture produced by condensation experiments in which grains are small and form fluffy and open aggregates consisting of hundreds and thousands of individual grains (Nuth et al., 2002; Rietmeijer et al., 2002).

4.3.2. The spinel fragments

With respect to spinels, their chemical trends (from Cr-rich to Al-rich, Fig. 8) may indicate the removal of Mg and Fe by being enclosed in olivine. The Al-content of spinel inclusions in olivine reflects both the liquid from which they originally crystallized and any subsequent reaction that occurred in a melt inclusion trapped in olivines. Our detailed study of all types of glasses present in D'Orbigny (Varela et al., 2003) show that those in primary glass inclusions trapped by olivine from the groundmass are Al-Ca-rich. However, glass inclusions do not co-exist with Al-rich spinels. Such spinels are present in D'Orbigny without glass. The only primary glass inclusion found in olivinite shows the co-existence of an Al-Ca-rich glass with a Cr-rich spinel (Fig. 6C). Thus spinel cores seem to be out of equilibrium with olivinites 2 and 4 with respect to Fe and Mg, with the atomic $Kd = (Mg/Fe)_{olivine}/(Mg/Fe)_{spinel}$ being about 5.5 and 6.5 for these pairs, respectively, far above the equilibrium value of ~2.5 (e.g., Kamenetsky et al., 2001). Only a spinel fragment in olivinite 1 with a Kd of about 2.9 is close to equilibrium. Spinels in olivinites seems to be in disequilibrium with the enclosing olivine, similar to that observed between spinel cores and olivine megacrysts or the cores of matrix olivines (e.g., Mittlefehldt et al., 2002; Kurat et al., 2004). Apparently, spinels are out of equilibrium with all enclosing olivines (olivinites, olivine megacrysts and olivine groundmass) in D'Orbigny. Co-existence of Cr-rich spinels with Mg-rich olivine is also observed in Azuka 881371 (Fig. 8) and in NWA 8535. In the latter, Cr-spinels are strongly zoned with parts of grains having substantial chromite grading into hercynite (Santos et al., 2016). A similar gradation towards hercynitic components was detected in the spinel fragment in olivinite 4 (Table 2).

The porous texture observed in the spinel fragments in olivinites, as well as the reaction zones that commonly cover spinels in the groundmass in D'Orbigny (described as "symplectic" texture by Mittlefehldt et al., 2002) and the strongly zoned spinels in NWA 8535 give evidence for a reaction affecting spinel. To date, we cannot firmly conclude if such a reaction took place before the spinels were captured by anorthite and/or olivine (e.g., Kurat et al., 2004) or after (e.g., Mittlefehldt et al., 2002). An answer to this question requires a detailed study of spinels in the different constituents of D'Orbigny. Such a study is underway.

4.3.3. Phase compositions

Olivinites in D'Orbginy are tightly intergrown with the host rock via anorthite, olivine and augite. The chemical composition of euhedral olivine crystals inside veins (e.g., olivine inside veins, Fig. 9A) shows a slight chemical variation as compared to those located close to veins (e.g., Olivine near veins, Fig. 9A). The latter overlap olivine grains that form the whole olivinite (e.g., Olivine, Fig. 9A). Olivines in the border zone have a Fa-rich composition ($Fa_{34.1}$) as compared to the Mg-rich olivine (~Fa_{10}, Table 1) (Figs. 9 and 10). There is a continuous increase of Fe and Mn from the Mg-rich olivine in olivinites to those forming the groundmass of D'Orbigny, which spread around the trend defined by the solar FeO/MnO ratio (Figs. 9A and 10). This primordial Fe/Mn ratio is also observed in olivine megacrysts from D'Orbginy and olivine grains from other angrites (e.g., Azuka 881371, Fig. 9A).

A similar increase in FeO and MnO contents is observed in augite grains (Fig. 9B). Those present in the border of the olivinites forming part of the reaction zone have a Fe/Mn ratio that overlaps the ratio measured in augites from the druses in D'Orbingy (Fig. 9B). All augites in D'Orbigny (e.g., present in olivinites, groundmass and druses), as well as those from other angrites, have a Fe/Mn ratio that follows the primordial ratio. Therefore, addition of Fe and Mn took place in a reservoir with chondritic proportion

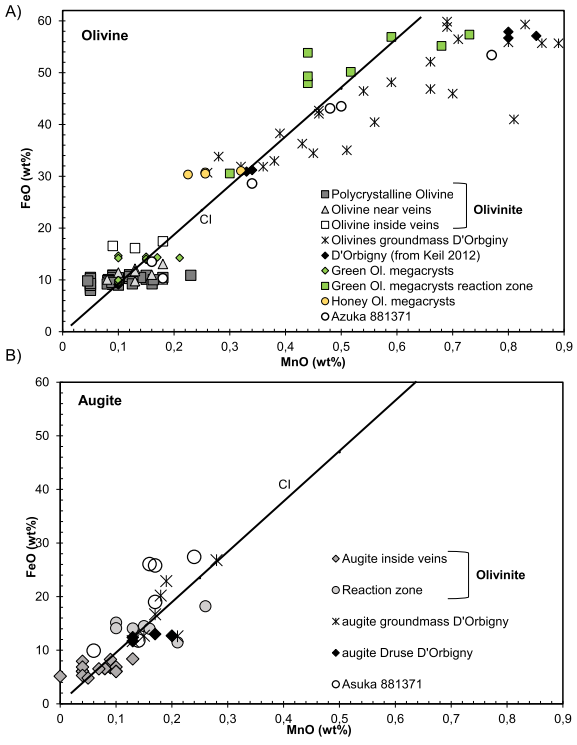

Fig. 9. FeO vs MnO diagram of: (A) All types of olivines in olivinites of D'Orbigny as well as olivine megacrysts (green [core and rim] and honey) and some olivines from the groundmass have FeO/MnO ratio spreading around the chondritic value (CI). Cl abundance ratio from Lodders and Fegley (1998). Olivines from angrite Asuka 881371 are given for comparison. (B) Augites in olivinites. Note that the FeO/MnO ratio of augites from inside veins and from the reaction zone in olivinites, as well as those from the groundmass and druse in D'Orbigny spread around the primordial ratio CI. Augites from angrites Asuka 881371 are given for comparison. (For interpretation of the references to colour in this figure legend, the reader is referred to the web version of this article.)

of these elements. A similar situation was previously observed in all types of glasses in D'Orbigny (see Fig. 12, Varela et al., 2003).

Apparently, major and minor phases in D'Orbigny keep a record of an exchange reaction which led to high FeO and MnO contents (Figs. 9 and 10C). The chondritic proportion of these elements indicates that this reaction took place in equilibrium with a chondritic reservoir. Only for high FeO contents (~50–60 wt%) the FeO/MnO ratio deviate from chondritic values (Fig. 10C). This trend is follow by olivines from the groundmass (Fig. 10A and B). Also, olivinites and groundmass olivines in D' Orbigny are characterized by highly variable CaO contents mainly for those having MnO contents higher than >0.5 wt% (Fig. 10D and E). Detailed EMPA study of these zones shows slight reverse zoning in mg# and CaO contents (Fig. 10A and B). Mikouchi et al. (2001) recognized this border zone as an overgrowth. This "reverse"-like profiles for FeO could be a direct consequence of the existence of Ca-Fe-olivine areas with adjacent low-Ca Fe-rich olivines zones, as discussed below.

4.3.3.1. The late Fe-Ca veneer. One of the latest events recorded by D'Orbigny produced the almost Mg-free mineral assemblage of Ca-rich olivine, kirschsteinite and titaniferous aluminous hedenbergite, all with atomic Fe/Mg ratios ~40 (Kurat et al., 2004). Olivine from the groundmass contains Ca with a core of $Fa_{35}La_1$, enveloped by a Fe-Ca-rich olivine zone partially replace by kirschsteinite ($Fa_{66}La_{33}$; Kirs, Fig. 11A). The Fe-Ca-rich olivine and kirschsteinite are not forming simple consecutive rims but are rather intergrown with each other in a complex way, filling the intergranular space. (Figs. 10A–B and 11A). Detailed zoning sequences in these phases in the groundmass of D'Orbigny show slight compositional reversals that cannot be explained by any mineralogical control in a closed system (Mittlefehldt et al., 2002). Accordingly, Mittlefehldt et al. (2002) invoked the addition of a more primitive melt during crystallization of D'Orbigny. However, a TEM study of the complex intergrowth of Ca-rich olivine and kirschsteinite area (Fig. 11A) reveals that the reaction zone is composed of well-defined domains of Fe-Ca-rich, Fe-rich and Ca-rich (Kirs) olivine (Fig. 11B). The complex intergrowth of these two phases separated by steep and abrupt compositional variations towards the rim (Fig. 10A and B), indicate that the Ca exchange may be due to a late-stage metasomatic process (Kurat et al., 2004) rather than a magmatic compositional zoning (Mittlefehldt et al., 2002). The steep compositional gradients between the Fo-rich core and Fa-rich overgrowths in olivinites, as well as the well-defined peaks in FeO and CaO abundances (Fig. 10A) and the slight reverse zoning (Fig. 10A and B), are evidence of such an event. We refer to it as the "Late Fe-Ca veneer". The co-existing Ca-rich olivine and kirschsteinite indicate a formation temperature of about 1000 °C (Davidson and Mukhopadhyay, 1984). At these high temperatures, the diffusion rates for Fe and Mg in olivine are very high. Hence, the preservation of well-defined domains (Fig. 11B) with abrupt compositional gradients across the plate edge in olivinites indicates that the late Fe-Ca veneer was a short-lived event in the history of this rock.

In summary, our results show that D'Orbigny experienced a metasomatic alteration process which was fed from a chondritic source (Figs. 9A–B and 10C) and led to enrichments (relative to the original composition) in FeO and MnO that established D'Orbigny's present-day composition. Therefore, the fayalitic content of the olivine from the groundmass in D'Orbigny (and possibly from many other angrites) may not be the original one. The recent finding of NWA 8535 containing 92% Mg-rich olivine (Santos et al., 2016) indicates that such olivines are not an exotic constituent in angrites. Olivinites and olivine megacrysts from D'Orbigny, as well as the Mg-rich olivines from Asuka 881371, NWA 1670 and NWA 8535 may represent the pristine olivines of angrites.

4.4. Links with chondritic constituents

One of the very early constituents of D'Orbigny could be the olivinites. Although they are mainly composed of fine-grained Mg-rich olivines, they also contain minor augites, anorthite and Cr-rich spinels, similar phases to those found

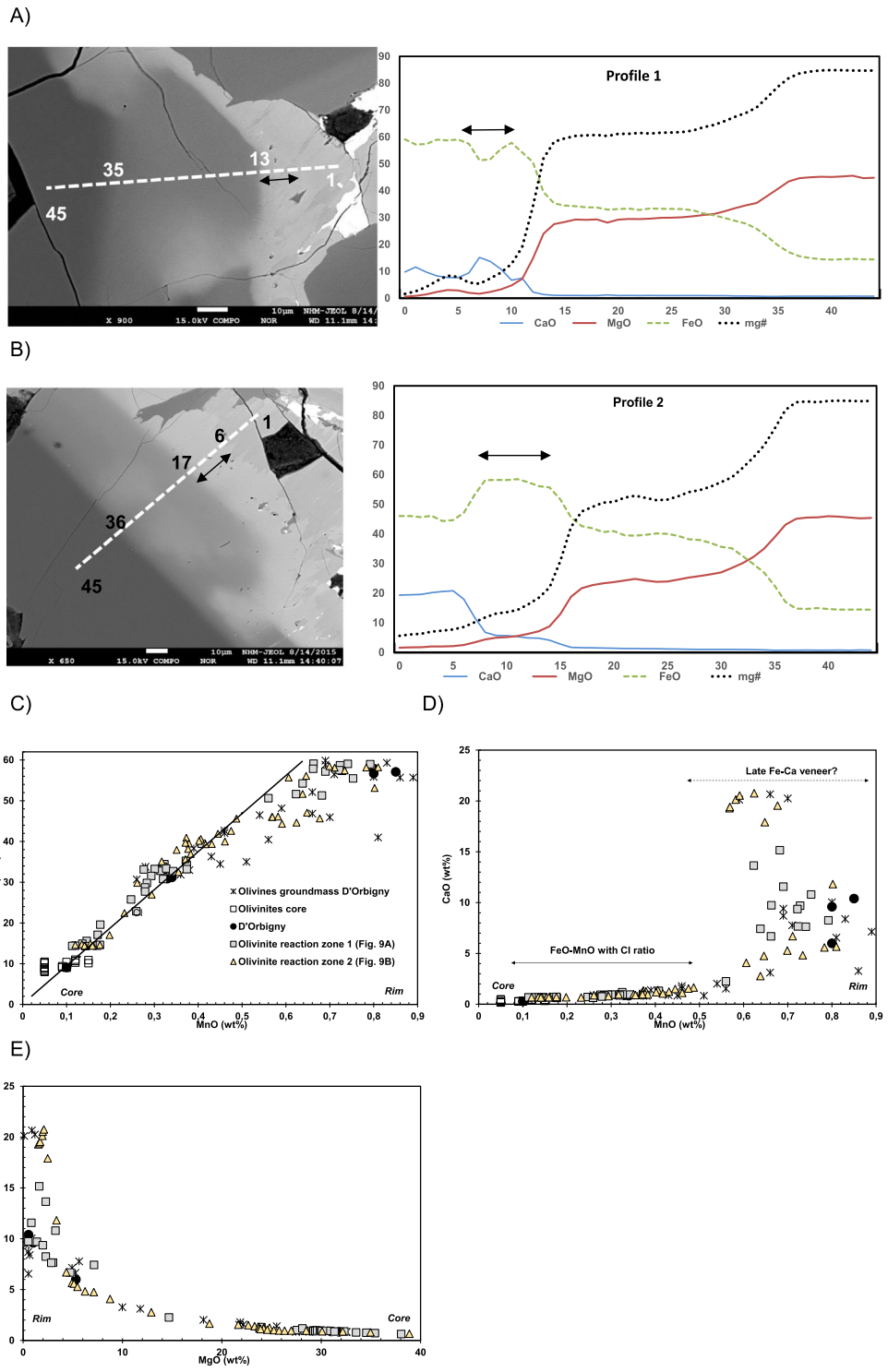

Fig. 10. (A-B) Back-scattered electron (BSE) images showing the reaction zone in olivinites. The white line (1–45) indicates a traverse along which 45 analyses of these zones were made (Profile 1 and 2). Intermediate numbers (13 and 35, Fig. 9A; 6, 17 and 36, Fig. 9B) indicate the beginning of each zone. The chemical variation in the profile (A) is as follow: 1 = Fa_{81}-Ca ol_{17}; 13 = $Fa_{63.1}$-Ca $ol_{3.61}$; 35 = Fa_{25}-Ca $ol_{0.7}$. In the profile (B) is: 1 = Fa_{62}-Ca $ol_{33.4}$; 6 = Fa_{59}-Ca $ol_{35.2}$; 17 = Fa_{56}-Ca $ol_{2.6}$; 36 = $Fa_{24.2}$-Ca $ol_{0.9}$. Variation of the FeO, CaO and MgO contents of these traverses are also shown in Profile 1 (A) and Profile 2 (B). Variation of the magnesium number (mg-no) is shown in Profile 1 (A). (C) FeO vs MnO binary diagram of the reaction zone of olivinites from Core to Rim. Note that all values spread around the primordial ratio and overlap the range of olivines from the groundmass in olivine. (D) CaO vs MnO binary diagram of the reaction zone from Core to Rim. Note the highly variable contents of CaO for MnO > 0.5 wt%. This area correspond to the so-called "Fe-Ca veneer". (E) CaO vs MgO binary diagram of the reaction zone from Rim to Core. Note the steep and abrupt increment in CaO for low MgO contents.

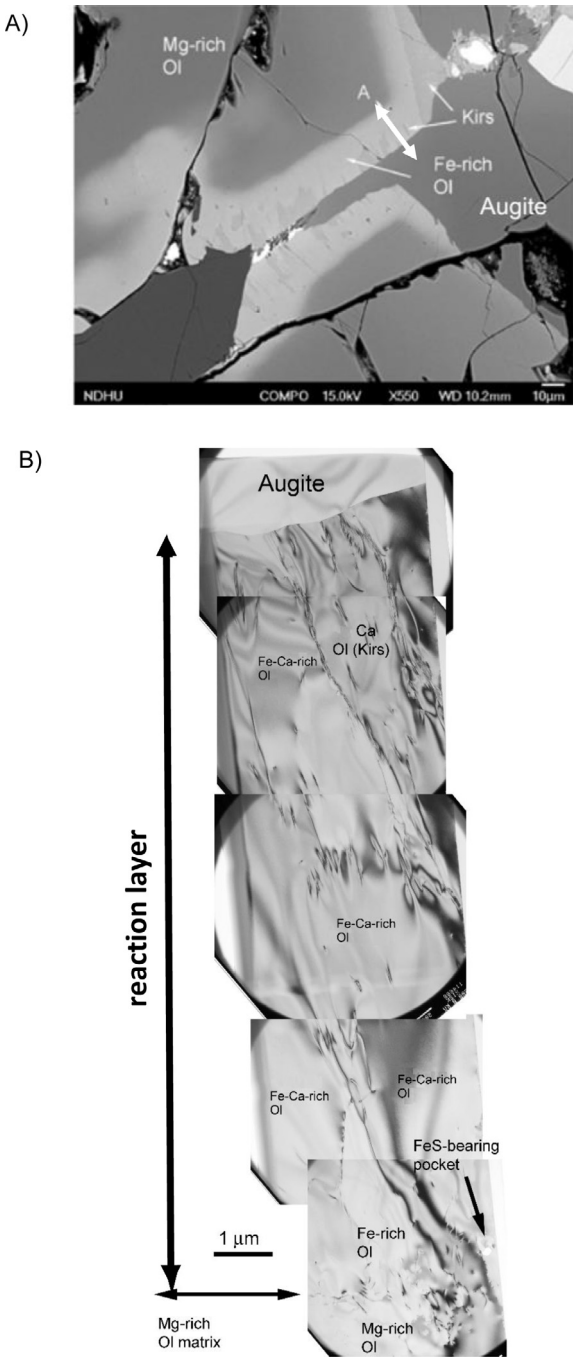

Fig. 11. (A) EBSE image showing the reaction zones surrounding olivines from D'Orbigny groundmass and the location of the FIB section (A) for TEM studies. Kirs: refers to kirschsteinite. (B) A TEM montage bright field image showing well developed domains of Fe-Ca-rich and Ca-rich (Kirs) olivine.

in NWA 8535. Formation of fine-grained olivinites or coarse-grained rocks (e.g., NWA 8535) might depend mainly on local growth conditions.

If these Mg-rich olivine rocks represent an early-formed cumulate derived from an angritic melt, as suggested for NWA 8535 (Santos et al., 2016), then the question arises: Can the observed mineralogy -with Mg-rich olivines as one of the first phases- be the result of precipitation from angritic melts?

There is no simple way to create a liquid of such particular composition. Prinz et al. (1988, 1990), Prinz and Weisberg (1995) and Longhi (1999) suggested that CAIs could have been the source of angritic liquids. Treiman (1989) also noted similarities in bulk composition of Angra dos Reis and CAIs. In addition, Longhi (1999) invoked a CAI component that had been mixed into a melt derived as a partial melt from an unknown but somehow chondritic precursor. This chondritic signature was preserved in the Fe/Mn ratio of the olivinites, olivine megacrysts, augite grains in olivinites and olivine forming the groundmass of D' Orbigny. It was also well-preserved in glasses, with not only the FeO/MnO ratio but also the FeO and MnO abundances being similar to those in CI chondrites (Varela et al., 2003). The presence of volatile elements such as carbon and nitrogen in glasses of glass inclusions and the refractory trace element abundances in glasses are also common features linking angrites and carbonaceous chondrites. Remarkably, D'Orbigny contains the trapped Xe-Q, a very primitive, chondritic Xe component (Busemann and Eugster, 2002) which cannot be expected to be preserved in silicate melts. However, a direct origin from chondritic rocks for angrites is constrained by the fact that angrites are alkali-free rocks. No chondritic rock without alkalis exists, but many CAIs carry this feature (Kurat et al., 2004). In addition, CAIs can have igneous as well as granoblastic textures and aggregation structures, similar to those observed in angrites. Nevertheless, an affinity of angrites to known CAIs appears to be not possible from an isotopic point of view (Lugmair et al., 1989), unless there was a generation of CAIs formed in a different reservoir to the ones we see in chondrites. The direct conclusion linking angrites with a special form of CAIs was mainly prevented by the high FeO and MnO contents of angrites as compared to the low ones of CAIs (Kurat et al., 2004). However, our results indicate that the high FeO and MnO might have a secondary origin. Therefore, from a chemical and petrological point of view, a relationship between angrites and CAIs cannot be ruled out.

5. CONCLUSIONS

Although angrites are considered to be igneous rocks of basaltic composition (Keil, 2012 and references therein), several lines of evidence point towards a possible CAIs-angrite relationship (Prinz et al., 1988, 1990; Prinz and Weisberg, 1995; Longhi, 1999; Kurat et al., 2004). One of the barriers to this straightforward conclusion is the high FeO and MnO contents of angrites. However, our results show that both elements have been added by a late metasomatic process that changed the initial Mg-rich composition of the olivines to the one we see now. As this process took place in equilibrium with a chondritic reservoir (e.g., Fe/Mn ratios spreading around primitive values), the primitive chemical composition (Mg-rich) was changed towards a more fayalitic one while preserving the chondritic signature. A late "Fe-Ca veneer", a short-lived event in the history of this rock,

might have produced the almost Mg-free mineral assemblage that characterized the angrite D'Orbigny (as well as other angrites). This metasomatic event may be related to the prevailing redox conditions which apparently became increasingly more oxidizing from one event to the other. The presence of high Ni-bearing metal and iron sulfide hosted by anorthite and anorthite + olivine gives clear evidence that the early events during D'Orbigny formation were reducing, possibly with high S activity (Varela et al., 2015). The first oxidizing event was efficient: it caused exchange of Mg for Fe in olivines. The relict composition of this event is only preserved in the olivinites and olivine megacrysts. On the other hand, the presence of FeS with $Fe_{1-x}O$-Fe_3O_4 core-shell crystals shows that the latest event was highly oxidizing (Hwang et al., 2015). These changing redox conditions were also recorded in olivinites with fragments showing abundant ribbon-like trails of multiphase [FeS_x + Fe-Ni metal + bubbles] inclusions and the existence of an additional weak doublet attributed to Fe^{3+}.

Since the discovery of the new angrite NWA 8535, which expands the range of known angrites lithologies to dunitic rocks (Agee et al., 2015), Mg-rich olivines might not be considered compositionally rare phases within these rocks. The large olivinites may represent vestiges of the pristine reducing conditions of the early history of angrites that in view of our results needs to be substantially revised.

ACKNOWLEDGEMENTS

We acknowledge D. Topa (NHM, Vienna) for assistance during microprobe analysis. Constructive reviews from Christine Floss, anonymous reviewers and the associated editor Sara Russel helped to considerably improve the manuscript. Financial support was received from FONCyT (PICT 0142) and CONICET (PIP 063), Argentina and the Ministry of Science and Technology, Taiwan, ROC.

REFERENCES

Abdu Y. A., Varela M. E. and Hawthorne F. C. (2011) Raman FTIR and Mössbauer spectroscopy of olivines from the D´ Orbigny meteorite. *Meteorit. Planet. Sci.* **46**(Suppl. A3) (abstr.).

Agee C. B., Miley H. M., Ziegler K. and Spilde M. N. (2015) Northwest Africa 8535: Unique Dunitic angrites. Lunar Planet. Sci. XLVI. Lunar Planet. Inst., Houston. #2681 (abstr.).

Amelin Y. (2008) U-Pb ages of angrites. *Geochim. Cosmochim. Acta* **72**, 221–232.

Bouvier A., Brennecka G. A., Sanborn M. E. and Wadhwa M. (2011) U-Pb chronology of newly recovered angrite. Lunar Planet. Sci. XLII. Lunar Planet. Inst., Houston. #2747 (abstr.).

Brennecka G. A., Wadhwa M., Janney P. E. and Anbar A. D. (2010) Towards reconciling early solar system chronometers: the $^{238}U/^{235}U$ ratios of chondrites and D'Orbigny pyroxenes. Lunar Planet. Sci. XLI. Lunar Planet. Inst., Houston. #2117 (abstr.).

Busemann H. and Eugster O. (2002) The trapped noble gas component in achondrites. *Meteorit. Planet. Sci.* **37**, 1865–1891.

Busemann H., Lorenzetti S. and Eugster O. (2006) Noble gases in D'Orbigny, Sahara 99555 and D'Orbigny glass—evidence for early planetary processing on the angrite parent body. *Geochim. Cosmochim. Acta* **70**, 5403–5425.

Davidson P. and Mukhopadhyay M. (1984) Ca-Fe-Mg olivines: phase relations and a solution model. *Contr. Mineral. Petrol.* **86**, 256–263.

Floss C., Crozaz G., McKay G., Mikouchi T. and Killgore M. (2003) Petrogenesis of angrites. *Geochim. Cosmochim. Acta* **67**, 4775–4789.

Glavin D. P., Kubny A. A., Jagoutz E. and Lugmair G. W. (2004) Mn-Cr isotope systematics of the D'Orbigny angrite. *Meteorit. Planet. Sci.* **39**, 693–700.

Hwang S. L., Chu H. T., Varela M. E., Yui T. F. and Shen P. (2012) SEM-EDX and ATEM studies of Olivinites from the angrite D'Orbigny. Meteorit. Planet. Sci. Suppl. #5124 (abstr.).

Hwang S.-L., Shen P., Chu H.-T., Yui T.-F., Iizuka Y. and Varela M. E. (2015) FeS grains with abundant $Fe_{1-x}O$-Fe_3O_4 core-shell crystals in the angrites D'Orbigny. Lunar Planet. Sci. XLVI. Lunar Planet. Inst., Houston. #1516 (abstr.).

Irving A. J., Kuehner S. M. and Rumble, III, D. (2008) Evidence for sulfur-rich fluids in the ancient angrite parent body. *Geochim. Cosmochim. Acta* **72**, A411 (abstr.).

Kamenetsky V. S., Crawford A. J. and Meffre S. (2001) Factors controlling chemistry of magmatic spinel: an empirical study of associated olivine, Cr-spinel and melt inclusions from primitive rocks. *J. Petrol.* **42**, 655–671.

Keil K. (2012) Angrites, a small but diverse suite of ancient, silica-undersaturated volcanic-plutonic mafic meteorites, and the history of their parent asteroid. *Chem. Erde* **72**, 191–218.

Kleine T., Hans U., Irving A. J. and Bourdon B. (2012) Chronology of the angrite parent body and implications for core formation in protoplanets. *Geochim. Cosmochim. Acta* **84**, 186–203.

Kurat G., Varela M. E., Brandstätter F., Weckwerth G., Clayton R., Weber H. W., Schultz L., Wäsch E. and Nazarov M. A. (2004) D'Orbigny: a non-igneous angritic achondrite. *Geochim. Cosmochim. Acta* **68**, 1901–1921.

Lodders K. and Fegley B. (1998) *The Planetary Scientist Companion*. Oxford University Press, 371 pp.

Longhi J. (1999) Phase equilibrium constraints on angrite petrogenesis. *Geochim. Cosmochim. Acta* **63**, 573–585.

Lugmair G. W., Galer S. J. G. and Loss R. (1989) Rb-Sr and other isotopic studies of the angrite LEW 86010. *Lunar Planet. Sci.* **20**, 604–605 (abstr.).

Mikouchi T. and McKay G. (2001) Mineralogical investigation of D'Orbigny: a new angrite showing close affinities to Asuka 881371, Sahara 99555 and Lewis Cliff 87051. Lunar Planet. Sci. XXXII. Lunar Planet. Inst., Houston. #1876 (abstr.).

Mikouchi T., Miyamoto M. and McKay G. A. (1996) Mineralogical study of angrite Asuka 881371: its possible relation to angrite Lew 87051. *Proc. Symp. Antarct. Meteorites* **9**(NIPR), 174–188.

Mikouchi T., Miyamoto M. and McKay G. (2001) Magnesian olivine xenocrysts in angrites Lewis Cliff 87051, Asuka-881371 and D'Orbigny: their relationship and origin. *Antarct. Meteor.* **26**, 80–82 (abstr.).

Mikouchi T., McKay G. A., Miyamoto M., Sugiyama K. (2011) Olivine xenocrysts in quenched angrites: the first "differentiated" materials in the solar system? Workshop on Formation of First Solids in the Solar System. Kawai, Hawaii, #1639 (abstr.).

Mittlefehldt D. W. and Lindstrom M. M. (1990) Geochemistry and genesis of theangrites. *Geochim. Cosmochim. Acta* **54**, 3209–3218.

Mittlefehldt D. W., Killgore M. and Lee M. T. (2002) Petrology and geochemistry of D'Orbigny, geochemistry of Sahara 99555, and the origin of angrites. *Meteorit. Planet. Sci.* **37**, 345–369.

Nuth, III, J. A., Rietmeijer F. J. M. and Hill H. G. (2002) Condensation process in astrophysical environments: the com-

position and structure of cometary grains. *Meteor. Planet. Sci.* **37**, 1579–1590.

Prinz M. and Weisberg M. K. (1995) Asuka 881371 and the angrites: origin in an heterogeneous, CAI-enriched, differentiated, volatile depleted body. *Antarct. Meteor.* **20**, 207–210.

Prinz M., Keil K., Hlava P. F., Berkley J. L., Gomes C. B. and Curvello W. S. (1977) Studies of Brazilian Meteorites, III. Origin and history of the Angra dos Reis achondrite. *Earth Planet. Sci. Lett.* **35**, 317–330.

Prinz M., Weisberg M. K., and Nehru C. E. (1988) LEW 86010, a second angrite: relationship to CAI's and opaque matrix. Lunar Planet. Sci. XIX. Lunar Planet. Inst., Houston. 949–950 (abstr.).

Prinz M., Weisberg M. K., and Nehru C. E. (1990) LEW 87051, a new angrite: origin in a Ca-Al-enriched eucritic planetesimal? Lunar Planet. Sci. XXI. Lunar Planet. Inst., Houston. 979–980 (abstr.).

Riches A. J. V., Day J. M. D., Walker R. J., Simonetti A., Liu Y., Neal C. R. and Taylor L. A. (2012) Rhenium–osmium isotope and highly-siderophile-element abundance systematics of angrite meteorites. *Earth Planet. Sci. Lett.* **353–354**, 208–218.

Rietmeijer F. J. M., Nuth, III, J. A. and Nelson R. N. (2002) Laboratory hydration of condensed magnesiosilicate smokes with implications for hydrated silicates in IDPs and comets. *Meteor. Planet. Sci.* **39**, 723–746.

Santos A. R., Agee C. B., Shearer C. K., and McCubbin F. M. (2016) Northwest Africa 8535 and Northwest Africa 10463: new insight into the angrites parent body. Lunar Planet. Sci. XLVII. Lunar Planet. Inst., Houston. #2590 (abstr.).

Schiller M., Connelly J. N., Glad Aslaug C., Mikouchi T. and Bizzarro M. (2015) Early accretion of protoplanets inferred from a reduced inner solar system 26Al inventory. *Earth Planet. Sci. Lett.* **420**, 45–54.

Treiman A. H. (1989) An alternate hypothesis for the origin of Angra dos Reis: porphyry, not cumulate. *Lunar Planet. Sci. Conf.* **19**, 443–450.

Varela M. E., Kurat G., Zinner E., Metrich N., Brandstaetter F., Ntaflos T. and Sylvester P. J. (2003) Glasses in the D'Orbigny angrite. *Geochim. Cosmochim. Acta* **67**, 5027–5046.

Varela M. E., Kurat G., Zinner E., Hoppe P., Ntaflos T. and Nazarov M. (2005) The non-igneous genesis of angrites: support from trace element distribution between phases in D´ Orbigny. *Meteorit. Planet. Sci.* **40**, 409–430.

Varela M. E., Hwang S.-L., Shen P., Chu H.-T., Yui T.-F., and Iizuka Y. (2015) High Ni-bearing metal and sulphide phases in the DOrbginy angrite. Lunar Planet. Sci. XLVI. Lunar Planet. Inst., Houston. #1497 (abstr.).

Warren P. H. and Kallemeyn G. W. (1995) Angrites—a volatile-rich variety of asteroidal basalt (except for alkalis and gallium). *Meteoritics* **30**, 593 (abstr.).

Warren P. H., Kallemeyn G. W. and Mayeda T. (1995) Consortium investigation of the Asuka 881371 angrite: bulk-rock geochemistry and oxygen isotopes. Antarctic Meteorites XX. NIPR, Tokyo. pp. 261–264.

Associate Editor: Sara S. Russell